

Infinite randomness critical behavior of the contact process on networks with long-range connections

Róbert Juhász

Institute for Solid State Physics and Optics, Wigner Research Centre for Physics,
H-1525 Budapest, P.O. Box 49, Hungary

E-mail: juhasz.robert@wigner.mta.hu

István A. Kovács

Institute for Solid State Physics and Optics, Wigner Research Centre for Physics,
H-1525 Budapest, P.O. Box 49, Hungary

E-mail: kovacs.istvan@wigner.mta.hu

Abstract. The contact process is studied on long-range connected networks in the presence of random transition rates by means of a strong disorder renormalization group method and Monte Carlo simulations. We focus on the case where the connection probability decays with the distance x as $p(x) \simeq \beta x^{-2}$ in one dimension. Here, the graph dimension of the network can be continuously tuned with β . The critical behavior of the model is found to be described by an infinite randomness fixed point which manifests itself in logarithmic dynamical scaling. Estimates of the complete set of the critical exponents, which are found to vary with the graph dimension, are provided by different methods. According to the results, the additional disorder of transition rates does not alter the infinite randomness critical behavior induced by the disordered topology of the underlying random network. This finding opens up the possibility of the application of an alternative tool, the strong disorder renormalization group method to dynamical processes on topologically disordered structures. As the random transverse-field Ising model falls into the same universality class as the random contact process, the results can be directly transferred to that model defined on the same networks.

1. Introduction

Dynamical processes occurring on random networks have been in the center of interest recently [1, 2]. The motivation of this field is many-sided, ranging from the spreading of epidemics or rumor in social networks via spreading of computer viruses to transportation networks [3]. There are at least two striking properties of the underlying networks in these problems which make the dynamics on the top of them much different from those on regular lattices. First, the nodes are “close” to each other, meaning that the number of nodes $n(\ell)$ that are reachable by traversing at most ℓ links from the origin is increasing rapidly with ℓ . In the case of an algebraic relationship

$$n(\ell) \sim \ell^{d_g}, \quad (1)$$

a generalized *graph dimension* can be associated with the network under consideration. In many cases in the above systems the graph dimension of the underlying network is formally infinite, like in the case of small world networks [4, 5] where, $\ln n(\ell) \sim \ell$, or in scale-free networks with a broad distribution of degrees, where $\ln[\ln n(\ell)] \sim \ell$ [3]. This “small-worldness” makes mean-field approximations successful in the description of phase transitions of spreading processes in many cases [6]. Second, the nodes of the underlying network are not equivalent since the degree of nodes, as well as the local neighborhoods are different and this circumstance may induce disorder effects on the dynamical process occurring on it. This issue has been recently studied [8, 9, 10] in the case of a paradigmatic model of an epidemic, the contact process [7]. In this model, there are binary variables attached to each node, which can be either active or inactive (infected or healthy in the parlance of epidemiology). Infected nodes then stochastically infect neighboring healthy nodes or recover. Varying the relative rates of these two competing processes the system can be driven from an active phase with a finite fraction of active nodes to an absorbing one where all sites are inactive. The phase transition on a translationally invariant lattice is known to fall into the directed percolation universality class [16, 17, 18]. This model has been studied on *long-range connected* (LRC) networks which consist of a d -dimensional hypercubic lattice and additional long-range edges existing with probability that decays algebraically with their Euclidean length x as $p(x) \simeq \beta x^{-s}$. This type of broad distribution of lengths of links has been observed in a mobile phone communication network, where $s = 2$ [11] and in the global airline network, where $s = 3$ [12]. The extremal cases $s = 0$ and $s = \infty$ correspond to small-world networks and short-range networks, respectively. In Refs. [8, 9, 10], where the case $d = 1$ was considered, the appearance of disorder effects was conjectured to be related with the finiteness of the graph dimension of the underlying network. This is realized in the $d = 1$ LRC network if the decay exponent s is large enough, $s \geq 2$ namely, which includes the “critical” point $s = 2$ where the graph dimension varies continuously with the prefactor β of the asymptotical probability of links ‡ [13, 14, 15].

‡ Note that, besides regular lattices, these networks provide an alternative for approaching the limiting case $d_g = \infty$ through tuning the prefactor β . Nevertheless, the two limiting cases may not be equivalent.

In this case, an anomalous slow, algebraic decay of the density of active nodes was observed in Monte Carlo simulations of the contact process in an extended phase on the subcritical side of the transition point, at least for small enough graph dimension. This region is an analogon of Griffiths-McCoy phase of disordered ferromagnets where the system, although it is globally paramagnetic, contains locally ferromagnetic domains of arbitrary size [19]. In the analogous phase of the contact process on LRC network, the majority of the system is locally sub-critical but the randomness of the structure leads to the formation of rare regions (sub-graphs) which contain an over-average number of internal links and, as a consequence, may be locally super-critical. The activity in these rare regions get extinct very slowly, so they give a large contribution to the average density and result in anomalous decay. The existence of this phase in the contact process with site-dependent random rates on regular lattices has been known for a long time [20]. In the following, we will term this type of inhomogeneity as *parameter disorder* in order to distinguish it from *topological disorder* which refers to the irregularities of the underlying network.

Besides the off-critical behavior, parameter disorder has a striking effect on critical scaling, as well [21], where, in the dynamical relations, the time is formally replaced by its logarithm. Indeed, an asymptotically exact *strong disorder renormalization group* (SDRG) treatment [23] of the one-dimensional model showed that, at least for sufficiently strong disorder, the critical behavior is controlled by an *infinite randomness fixed-point* (IRFP) where the temporal scaling is logarithmic and yielded the complete set of critical exponents [22]. Later, this type of critical scaling has been indicated by the SDRG method in higher dimensions $d = 2, 3, 4$, as well as on the Erdős-Rényi graph [24] (where formally $d_g = \infty$) with parameter disorder [25, 26, 27]. Based on these results, the existence of infinite-randomness critical behavior was conjectured on arbitrarily high-dimensional hypercubic lattices for sufficiently strong parameter disorder.

On LRC networks, where solely topological disorder is present, numerical simulations have indicated a logarithmic critical scaling for small enough graph dimension, where the critical exponents vary with d_g but a precise estimation of them is still lacking. Here, the critical point has been found to be flanked with a Griffiths phase, the width of which is shrinking with increasing d_g [8, 9, 10]. For larger d_g (from $d_g \approx 2$ on) a Griffiths phase could not be observed and the judgement of the critical behavior became less certain. Here the data were compatible with a conventional algebraic scaling.

In this paper, we wish to contribute to the above issue by revisiting some still unclear parts, as well as to extend it to another direction. Namely, we shall focus on the critical behavior of the contact process on $d = 1$ LRC networks but, as a new feature, mainly *in the presence of parameter disorder*. Keeping in mind the universality of the IRFP in case of parameter disorder, meaning that the critical exponents are independent of the distribution random parameters [23], we pose the question whether, on a structure with topological disorder, the critical exponents of the transition are modified by an additional parameter disorder or not. A methodological yield of this new component

is that the model becomes eligible for a SDRG analysis that always necessitates some initial parameter disorder. Furthermore, we expect the additional parameter disorder enhancing the effective strength of disorder (i.e. reducing the transient regimes which are usually rather long in the IRFP) and making possible a more accurate numerical investigation. We shall thus perform a numerical SDRG analysis of the above model and compare the predictions with results of Monte Carlo simulations.

It is worth mentioning that, provided it is controlled by an IRFP, the transition of the disordered contact process falls into the same universality class as that of the random transverse-field Ising model on any structure, as the strong disorder renormalization rules of the two models are identical (apart from factors that are irrelevant at criticality) [30]. Besides regular lattices, the (zero-temperature) quantum phase transition in this model has been studied also on a LRC network when the underlying network is driven through a (long-range) percolation transition [31]. Here, the critical exponents of the model can be expressed in terms of those of the percolation transition. However, the nature of the quantum phase transition controlled by the strength of the transversal field (on the percolating LRC network), which is a much harder problem, and which is the subject of this work, has not been revealed yet. Due to universality, the results of our investigations can immediately be transferred to the quantum critical behavior of the random transverse-field Ising model.

The rest of the paper is organized as follows. The precise definition of the model will be given in section 2. In section 3, the scaling theory of the IRFP will be recapitulated. Section 4 is devoted to the SDRG analysis of the critical behavior, while results of Monte Carlo simulations are presented in section 5. Finally, the results are discussed in section 6 and conclusions are drawn in section 7.

2. The model

Networks with an algebraically decaying probability of long edges have been studied in the past from different aspects. In addition to the examples mentioned so far, they also arise as models of linear polymers with crosslinks between remote monomers [32], in the context of decentralized search algorithms [33], or, indirectly, in susceptible-infected-recovered models with long-range infection [38]. Besides contact process [8, 9, 10], long-range percolation [35], random walks [36, 15], susceptible-infected-recovered model [37] and spin glass models [34] have been studied on them. The geometry of these networks itself (the dependence of the diameter on the number of nodes) has attracted much interest, as well [13, 39, 40, 14, 41, 42, 38].

Concerning the precise definition of the LRC networks, we shall adopt that of Ref. [13]. Let us have a set of N nodes, which are labeled by integers $1, 2, \dots, N$ and define the distance between node i and j as $x_{ij} = \min(|i - j|, N - |i - j|)$. This simply means that the nodes are arranged on a ring with unit spacing between them. Then all pairs of nodes with a distance $x_{ij} = 1$ (i.e. neighboring nodes on the ring) are connected with

a link and all pairs with $x_{ij} > 1$ are connected independently with the probability

$$p(x) = 1 - \exp(-\beta x^{-s}), \quad (2)$$

where β and s are positive constants. For large x , this probability has the asymptotic form

$$p(x) \simeq \beta x^{-s}. \quad (3)$$

A finite realization of this network is illustrated in Fig. 1.

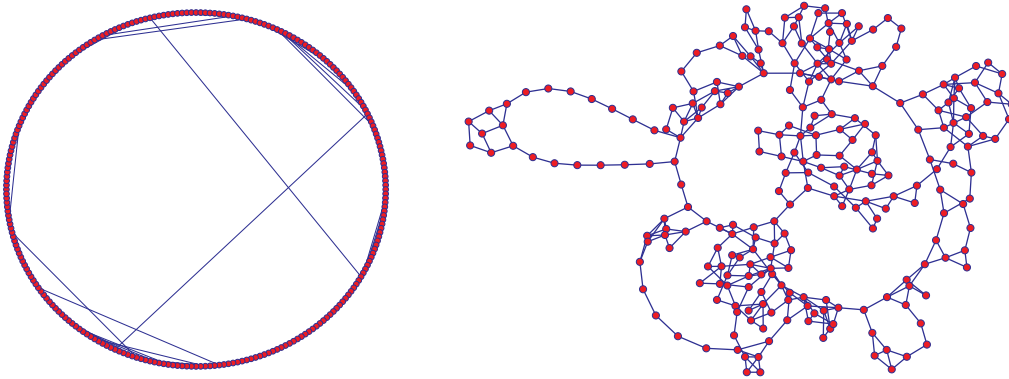


Figure 1. Left: A realization of the LRC networks with $N = 256$ and $\beta = 1$. Right: The same network represented with roughly equal edge lengths visualized by the Pajek program [43].

As for the geometry of these networks, for our purposes it is sufficient to know that if $s = 2$, the graph dimension is finite and continuously increasing with β from one to infinity [13, 14], for numerical estimates, see Refs. [15, 38]. If $s > 2$, the network is short-ranged (i.e. $d_g = 1$), whereas if $s < 2$, formally $d_g = \infty$ that hides in the range $1 < s < 2$ an increase of the diameter with a power of $\ln N$ [41]. In the present work, we shall restrict ourselves to the critical value $s = 2$.

To the nodes of these networks binary variables n_i coding active ($n_i = 1$) and inactive ($n_i = 0$) states are attached, and on this state space a continuous-time stochastic process is considered with the following transitions. If node i is active it can become inactive with a rate μ_i , as well as it tries to activate each neighboring node j with a rate λ_{ij} . The rates μ_i and λ_{ij} are i.i.d. quenched random variables drawn from a distribution that will be specified later.

Note that the homogeneous version of this model, where $\mu_i = \mu = \text{const}$, $\lambda_{ij} = \text{const} = \lambda$ is known as the susceptible-infected-susceptible (SIS) model rather than the contact process. In the former model the infection rates on links whereas in the latter the total rate of infection from nodes are constant. In other words, in the

homogeneous contact process, the rate of infection from node i through a given link is λ/d_i , where d_i is the coordination number (or degree) of node i . Therefore, in the case of the contact process on a non-regular lattice the infection rates on a given link can be different in the two directions. Although this situation is tractable by the SDRG method [44], an efficient algorithm is at our disposal that works for the symmetric case, thus the SDRG analysis will be carried out for the SIS model. In computer simulations, however, it is more natural to implement the contact process rather than the SIS. (For the discrete time-implementation see section 5.) Nevertheless, in the case of networks with a narrow distribution of degrees, which is the case for the LRC networks with an asymptotically N -independent distribution, the above distinction between the two models is irrelevant as far as the critical exponents are concerned.

3. Scaling theory in an IRFP

Here, following mainly Ref. [22], we shall briefly recapitulate the essentials of the scaling at an infinite randomness fixed-point, in a form adapted to finite-dimensional networks.

As it is natural in strongly disordered systems [23], we define the control parameter in the form $\Delta_0 \equiv \overline{\ln(\lambda/\mu)}$, where the over-bar denotes an average over the distribution of rates, whereas $\Delta \equiv \Delta_0 - \Delta_0^*$ will denote the deviation from the critical value Δ_0^* . As we will formulate the scaling theory for random networks, the usual linear size appearing in scaling relations will be replaced by the mean diameter D of networks with N nodes.

An appropriate order parameter of the transition is the probability ρ that a randomly chosen node in the stationary state of the infinite system ($N \rightarrow \infty$) is active. In the active phase and close to the critical point it vanishes as

$$\rho(\Delta) \sim \Delta^\beta, \quad (4)$$

defining the order parameter exponent β . Close to the transition, the spatial correlation length (measured in terms of the Euclidean distance x), ξ_\perp diverges as

$$\xi_\perp \sim |\Delta|^{-\nu_\perp}, \quad (5)$$

with the correlation length exponent ν_\perp . The dynamics in an IRFP are strongly anisotropic; the time and length scales are, namely, related to each other as

$$\ln \xi_\parallel \sim \xi_\perp^\psi, \quad (6)$$

where ψ is the tunneling exponent and plays the role of a dynamical exponent. Note that the conventional dynamical exponent that is defined by an algebraic relationship rather than Eq. 6 is formally infinite here. Based on the above, the order parameter for finite size D and time t is expected to have the scaling form when the length (measured in shortest-path distance ℓ) is rescaled by a factor b as:

$$\rho(D, t, \Delta) = b^{-x} \tilde{\rho}(D/b, \ln t/b^\psi, \Delta b^{1/\nu_\perp}), \quad (7)$$

where $x \equiv \beta/\nu_\perp$.

The observables the time-dependences of which are usually measured in numerical simulations starting from a single active node are the survival probability, the average

number of active nodes and the spread [16]. The first one is the probability that there will be at least one active node at time t . This probability is then averaged over the position of the initial active seed. For the contact process, it scales in the same way as the order parameter [17, 18] so we have

$$P(D, t, \Delta) = b^{-x} \tilde{P}(D/b, \ln t/b^\psi, \Delta b^{1/\nu_\perp}). \quad (8)$$

Writing a scaling relation for the spatio-temporal correlation function $C[n_0(t=0), n_i(t)]$ analogous to Eq. (7) then summing over the position i yields for the scaling of the average number of active nodes:

$$N_a(D, t, \Delta) = b^{d_g - 2x} \tilde{N}(D/b, \ln t/b^\psi, \Delta b^{1/\nu_\perp}). \quad (9)$$

The spread is usually defined as the root-mean-square of the Euclidean distance of active nodes from the origin. This quantity would, however, diverge in our model for $s \leq 2$ owing to the long links, therefore we define it in terms of the shortest-path distance ℓ as

$$R(t) = \sqrt{\langle \sum_i n_i(t) \ell_i^2(t) / \sum_i n_i(t) \rangle}, \quad (10)$$

where $\langle \cdot \rangle$ denotes the expected value conditioned on the survival up to time t for a given random environment (i.e. a given random network and given starting position) whereas the overbar denotes an average over the latter. Using again the scaling form of the spatio-temporal correlation function one obtains that the spread obeys the scaling relation

$$R(D, t, \Delta) = b \tilde{R}(D/b, \ln t/b^\psi, \Delta b^{1/\nu_\perp}). \quad (11)$$

In the critical point ($\Delta = 0$) of the infinite system ($D = \infty$) it follows from the above relations that the observables depend on time asymptotically as

$$P(t) \sim [\ln(t/t_0)]^{-\bar{\delta}}, \quad (12)$$

$$N_a(t) \sim [\ln(t/t_0)]^{\bar{\eta}}, \quad (13)$$

$$R(t) \sim [\ln(t/t_0)]^{1/\psi}, \quad (14)$$

where t_0 is a non-universal microscopic time-scale and the exponents are given in terms of the earlier ones as

$$\bar{\delta} \equiv x/\psi, \quad \bar{\eta} \equiv (d_g - 2x)/\psi. \quad (15)$$

A further quantity that is directly accessible by the SDRG method is the lowest gap ϵ of the rate matrix (or infinitesimal generator) of the process in finite systems (see the next section). This quantity varies from sample-to-sample and can be interpreted as the inverse of the mean time τ needed to reach the absorbing state starting from the fully active one in a given finite sample. The distribution of its logarithm in samples with fixed N , in the critical point $\Delta = 0$ obeys the finite-size-scaling relation

$$f_\epsilon(\ln \epsilon, D) = D^{-\psi} \tilde{f}_\epsilon(D^{-\psi} \ln \epsilon). \quad (16)$$

Similarly, the distribution of mean lifetime τ has the scaling form

$$f_\tau(\ln \tau, D) = D^{-\psi} \tilde{f}_\tau(D^{-\psi} \ln \tau). \quad (17)$$

Note that, in the above scaling relations, we could have equally well used the “volume” N of networks instead of their diameter D . But in that case, as it is easy to see from the relation $D(N) \sim N^{1/d_g}$, the scaling exponents involving the finite size would differ from the present ones by a factor of $1/d_g$ and the graph dimension in Eqs. (9,15) should be replaced by 1. This set of exponents defined in terms of the volume will be distinguished by a prime from the above ones:

$$\psi' \equiv \psi/d_g, \quad x' \equiv x/d_g, \quad \nu' \equiv \nu d_g. \quad (18)$$

The other exponents are not effected by the choice of the measure of the size.

4. SDRG treatment

By the SDRG procedure, the quickly relaxing degrees of freedom – that are related to high-lying levels of the rate matrix that governs the time-evolution – are sequentially eliminated, while lower-lying levels which are responsible for the long-range dynamics are kept [22].

To be specific, the procedure consists of two kinds of reduction steps. First, if the infection rate λ_{ij} on a link is much greater than the recovery rates on nodes i and j then the two nodes are merged and treated as a single giant node with the effective recovery rate

$$\tilde{\mu} \simeq 2\mu_i\mu_j/\lambda_{ij} \quad (19)$$

and size $\tilde{m} = m_i + m_j$. Second, if the recovery rate μ_i on node i is much greater than the infection rates on the links emanating from it then node i is eliminated while any pairs of nodes neighboring to it are connected by new links with effective infection rates

$$\tilde{\lambda}_{jk} \simeq \lambda_{ji}\lambda_{ik}/\mu_i \quad (20)$$

on them.

In the original formulation of the SDRG scheme the largest transition rate is selected then either of the above reduction steps are applied and this loop is iterated until the system is sufficiently small so that the spectrum of the rate matrix can be directly calculated. Although the reduction steps are approximative, they become more and more accurate as the renormalization proceeds since the distributions of logarithmic rates broaden without limits, and ultimately, the method becomes asymptotically exact in the IRFP [30, 23].

This renormalization scheme is formally equivalent to that of the random transverse-field Ising model defined by the Hamiltonian

$$H = - \sum_{\langle ij \rangle} J_{ij} \sigma_i^x \sigma_j^x - \sum_i h_i \sigma_i^z, \quad (21)$$

where $\sigma_i^{x,z}$ are Pauli operators on site i , J_{ij} and h_i are random couplings and external fields, respectively, and the first sum goes over neighboring nodes of the network [30]. The asymptotic renormalization rules of the model take the forms given in Eqs. (19,20) with the correspondences $\mu_i \leftrightarrow h_i$ and $\lambda_{ij} \leftrightarrow J_{ij}$, apart from the absence of the factor of 2 in Eq. (19), which, however, does not influence the critical exponents at an IRFP.

The performance of the SDRG method in the above form may be rather ineffective in other than one dimension since the connectedness of the underlying network will rapidly increase by the renormalization. To avoid this we will use a more efficient algorithm developed by one of us [26, 28], which is based on the so called 'maximum rule'. According to this, if multiple links between nodes would appear during the renormalization, only the one with the maximal rate is kept. Application of this rule is thought not to influence the critical exponents at an IRFP and results in simplifications of the SDRG procedure. The improved algorithm works by merely deleting links (and changing the rates on the remaining ones), without generating new ones at all. The results of the algorithm are identical to that of any traditional implementation of the SDRG method (having also the widely applied maximum rule) for any finite graphs, with N sites and E edges. However, we gain considerable time in performance: while the traditional method needs $\mathcal{O}(N^3)$ operations, the improved algorithm requires only $\mathcal{O}(N \log N + E)$, which is in practice much faster, than the $\mathcal{O}(N^2)$ operations needed to generate the LRC networks. The essence of the algorithm is that if two (or more) sources are able to infect each other mutually before being healthy again, than these form a new effective infection source, for which it takes a longer time to become healthy again. So, in this sense, the process can be regarded as a special kind of percolation of the infection sources with a positive feedback [26, 28].

In the numerical SDRG analysis, both variables λ_{ij} and μ_i where taken from uniform distributions with probability densities $f_\lambda(\lambda) = \Theta(\lambda)\Theta(1 - \lambda)$ and $f_\mu(\mu) = \frac{1}{\mu_m}\Theta(\mu)\Theta(\mu_m - \mu)$, respectively, where $\Theta(x)$ is the Heaviside step-function and we used the logarithmic variable, $\Delta_0 = \ln(\mu_m)$ as a control parameter.

It is generally a challenging task to precisely locate the critical point, and the accuracy of the obtained critical exponents depends crucially on it. In order to reach a sufficient precision, we have first determined the location Δ_c of the pseudo-critical point for each random sample, where the correlation length reaches the size of the system. This can be conveniently obtained by the doubling method [29, 28]. Here, the originally periodic system is made "open" by cutting all links going over a given position x , and two identical copies of this open system are glued together at the boundaries. Then, Δ_c is given by the threshold value, above which the last remaining giant nodes (or clusters) of the replicas fuse together during the SDRG process. Δ_c varies from sample to sample, but from the size-dependence of its distribution both the location Δ_0^* of the 'true' critical point and the correlation length exponent ν' can be obtained according to the scaling form:

$$f_\Delta(\Delta, N) = N^{1/\nu'} \tilde{f}_\Delta(\Delta N^{1/\nu'}), \quad (22)$$

where $\Delta = \Delta_c - \Delta_0^*$. In practice, we study the scaling of the width of the distribution (given by the standard deviation), which is proportional to $N^{-1/d_g\nu}$ and the mean value, $|\Delta_0^* - \overline{\Delta_c}| \sim N^{-1/d_g\nu}$, and calculate size-dependent effective exponents by two-point and three-point fits, which are then extrapolated as $1/N \rightarrow 0$, see Fig. 2.

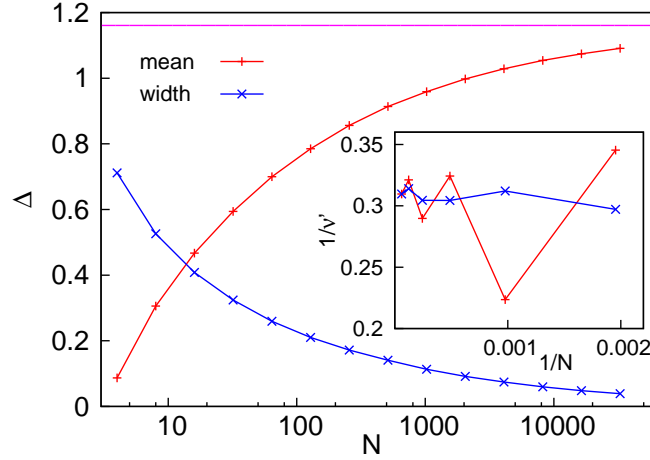


Figure 2. The distribution of the pseudo-critical points at $\beta = 0.75$ is illustrated by the mean value and the width of the distribution for various values of the system size N . The extrapolated value of the critical point is $\Delta_0^* = 1.1606(15)$, indicated by the solid line. Inset: The obtained finite-size estimates of the exponents $1/\nu'$ lead to the asymptotic value $1/\nu' = 0.308(8)$.

Having at hand an accurate estimate for the location of the critical point, the remaining two independent critical exponents (x' and ψ') can be determined by applying the SDRG method at the critical point and analyzing the resulting cluster structure. The gap ϵ of the rate matrix (or energy gap in the language of the Ising model) is given by the effective recovery rate of the the last decimated giant node (cluster). The mass m of the latter gives the magnetic moment of the sample in the corresponding Ising model, for details, see [25, 26, 28]. The number of independent random samples used in the calculations were at least 40000, while the largest analyzed system size was typically $N = 2^{15}$.

According to the scaling theory presented in the previous section, the average mass scales with N as $m(N) \sim N^{1-x'}$, since it is related to the order parameter (magnetization of the Ising model) ρ as $\rho = m/N$. This is illustrated in Fig.3 for $\beta = 0.75$. For sufficiently large system sizes, the points fit well to a straight line. From two-point fits we can obtain finite-size estimates of $1 - x'$, which is then extrapolated as $1/N \rightarrow 0$.

The mean value and the width of the distribution of $\ln \epsilon$ is shown in Fig.4 for $\beta = 0.75$. As a clear indication of infinite disorder scaling, the width of the distribution is increasing with N . According to the scaling form in Eq. 16, both the mean value and the width is asymptotically proportional to $N^{\psi'}$. Similarly to the other exponents, we determined finite-size estimates for ψ' through two-point fits, as illustrated in the inset

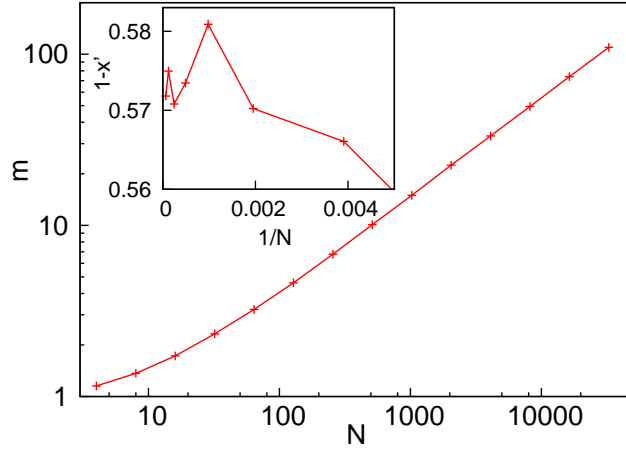


Figure 3. The average mass of the last cluster as the function of the system size, N at $\beta = 0.75$. Inset: The obtained finite-size estimates of $1 - x'$ lead to the asymptotic value $1 - x' = 0.575(10)$.

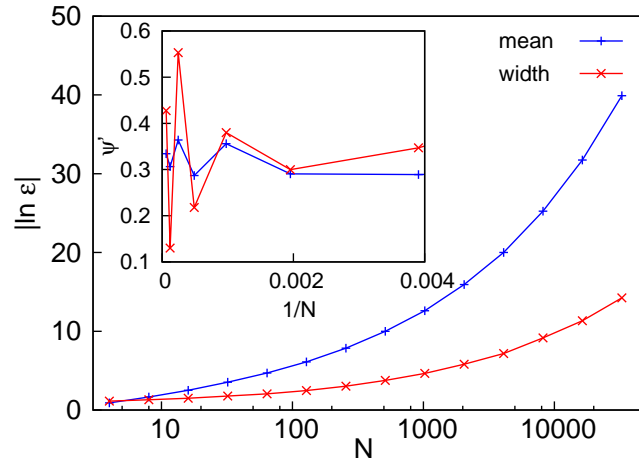


Figure 4. The mean value and width of the distribution of the logarithmic gap plotted against the system size N for $\beta = 0.75$. Inset: The obtained finite-size estimates of ψ' lead to the asymptotic value $\psi' = 0.32(3)$.

of Fig. 4. The estimates obtained by extrapolations to $N \rightarrow \infty$ are presented in Table 1.

5. Monte Carlo simulations

We have performed Monte Carlo simulations of the contact process on LRC networks, implemented in the following way. A finite LRC network with N nodes with i.i.d. random variables $w_{ij} = w_{ji}$ on each link have been generated. Choosing an active node (i) randomly, it is set to inactive with a probability $1/(1 + \lambda)$. Otherwise, a neighboring

β	d_g	Δ_0^*	$1/\nu'$	x'	ψ'	ψ
0.1	1.104(2)	0.1738(4)	0.422(7)	0.214(3)	0.524(30)	0.58(3)
0.2	1.212(4)	0.3505(5)	0.366(4)	0.231(5)	0.53(3)	0.64(4)
0.3	1.353(7)	0.529(2)	0.323(10)	0.264(6)	0.525(20)	0.71(3)
0.4	1.499(7)	0.700(1)	0.301(6)	0.291(10)	0.485(30)	0.73(5)
0.5	1.656(8)	0.856(1)	0.295(8)	0.329(7)	0.448(35)	0.74(6)
0.75	2.03(2)	1.1606(15)	0.308(8)	0.426(8)	0.33(3)	0.67(6)
1.0	2.347(17)	1.3685(10)	0.333(10)	0.469(6)	0.277(17)	0.65(4)
2.0	3.045(27)	1.853(3)	0.335(4)	0.531(10)	0.22(4)	0.67(12)

Table 1. Critical exponents estimated by the SDRG method for different values of β . The graph dimensions are taken from Ref. [15]; for more precise estimates, see Ref. [38].

node (j) is chosen equiprobably and it is activated with a probability w_{ij} (provided it was previously inactive). The random variables w_{ij} have been drawn from a discrete, binary distribution with probability density $f(w) = c\delta(w - w_0) + (1 - c)\delta(w - 1)$. This can be interpreted in a way that a fraction c of the links has a reduced capacity of transmitting the disease that is characterized by the parameter $w_0 < 1$. The parameters of this distribution have been chosen to be $c = 0.5$ and $w_0 = 0.2$ throughout the numerical simulations, except of the homogeneous model (i.e. the model without parameter disorder) where formally $c = 0$. One Monte Carlo step of unit time consists of $N_a(t)$ such updates where $N_a(t)$ is the number of active nodes at the beginning of the step. We have generated random networks with a fixed β in the range $[0.2, 2]$ and with $N = 1 - 5 \cdot 10^6$ nodes (larger ones for larger d_g) and – starting with a single active seed – we have simulated the process and measured the survival probability, the number of active nodes and the spread as a function of time, typically, for MC times up to 2^{20} . This measurement has been repeated for a fixed β and λ in 10^2 independent random networks, starting the process from 10^4 different nodes per sample, and the measured data have been averaged. When presenting results of the Monte Carlo simulations, we will simply use λ as a control parameter rather than Δ_0 defined in section 3.

The critical point have been estimated in the way proposed in Ref. [45] in order to avoid the difficulties about the large time scale t_0 in Eqs. (13). Plotting $\ln N_a(t)$ against $\ln P(t)$, the slope of the curve must tend to $+1$ in the inactive phase, to $-\bar{\eta}/\bar{\delta}$ in the critical point, and to $-\infty$ in the active phase, see Fig. 5. Having identified the critical point for different β , we have determined $\bar{\eta}/\bar{\delta}$ by a linear fit to the critical curve, see Fig. 6. Using Eqs. (15,18), the exponent x' has then been calculated from

$$x' = 1/(2 + \bar{\eta}/\bar{\delta}). \quad (23)$$

The estimates obtained this way are given in Table 2. Note that the most significant source of the error comes from the uncertainty of the critical point.

The tunneling exponent ψ has been determined from the dependence of the spread

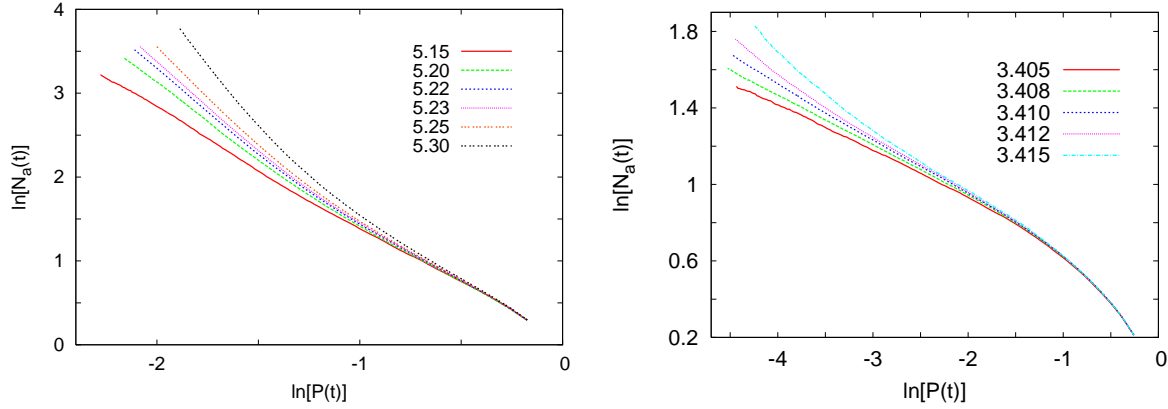


Figure 5. The logarithm of the average number of active nodes plotted against the logarithm of the survival probability for different values of λ for $\beta = 0.3$ (left) and $\beta = 1$ (right). The critical point is located at $\lambda^* = 5.22(1)$ for $\beta = 0.5$ and at $\lambda^* = 3.408(3)$ for $\beta = 1$.

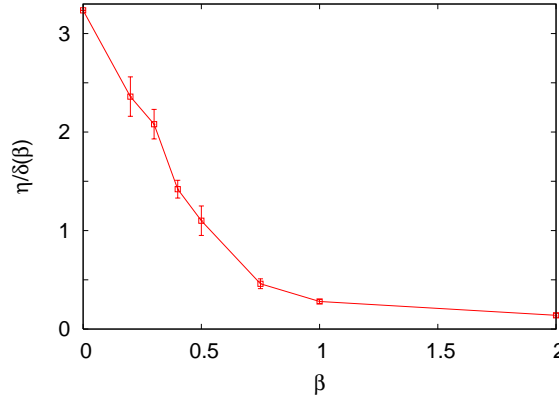


Figure 6. The ratio of exponents η/δ measured in Monte Carlo simulations for different values of β . The value at $\beta = 0$ is the SDRG prediction for the one-dimensional random contact process [22].

on time by fitting a function $R(t) = a[\ln(t/t_0)]^{1/\psi} + b$ to the numerical data for times $\ln t > 5$. For an illustration, see Fig. 7. The estimates for various β can be found in Table 2. For $\beta = 1$, we have determined the tunneling exponent also by measuring the lifetime τ starting from a fully active initial state in finite systems. Constructing the histogram of $\ln \tau$ for different values of N , the exponent ψ can be determined, according to Eq. (17), by finding an optimal scaling collapse of the data, see Fig. 7. The obtained estimate ($\psi' = 0.23$) is compatible with that obtained from the time-dependence of the spread. As can be seen in Fig. 8, the dependence of the survival probability and the average number of active nodes on time is in agreement with the logarithmic scaling laws given in Eqs. (12,13).

In addition to this, we have performed simulations and measurements for model without parameter disorder (i.e. formally $c = 0$), as well, in the same way as for the

β	d_g	λ^*	$\bar{\eta}/\bar{\delta}$	x'	ψ	λ^* ($c = 0$)	$\bar{\eta}/\bar{\delta}$ ($c = 0$)	ψ ($c = 0$)
0.2	1.212(4)	5.83(1)	2.36(20)	0.229(10)	0.57(5)	2.855(10)	2.3(3)	0.55(5)
0.3	1.353(7)	5.22(1)	2.08(15)	0.245(9)				
0.4	1.499(7)	4.70(1)	1.42(9)	0.292(8)				
0.5	1.656(8)	4.32(1)	1.10(15)	0.323(16)	0.56(8)			
0.75	2.03(2)	3.728(5)	0.46(5)	0.407(8)	0.60(8)	2.116(1)	0.45(5)	
1.0	2.347(17)	3.408(3)	0.28(2)	0.439(4)	0.53(5)	1.976(1)	0.26(5)	0.52(7)
2.0	3.045(27)	2.850(5)	0.14(2)	0.467(4)				

Table 2. Critical exponents estimated by Monte Carlo simulations for different values of β . The graph dimensions are taken from Ref. [15]. Estimates in the absence of parameter disorder ($c = 0$) are shown in the last three columns.

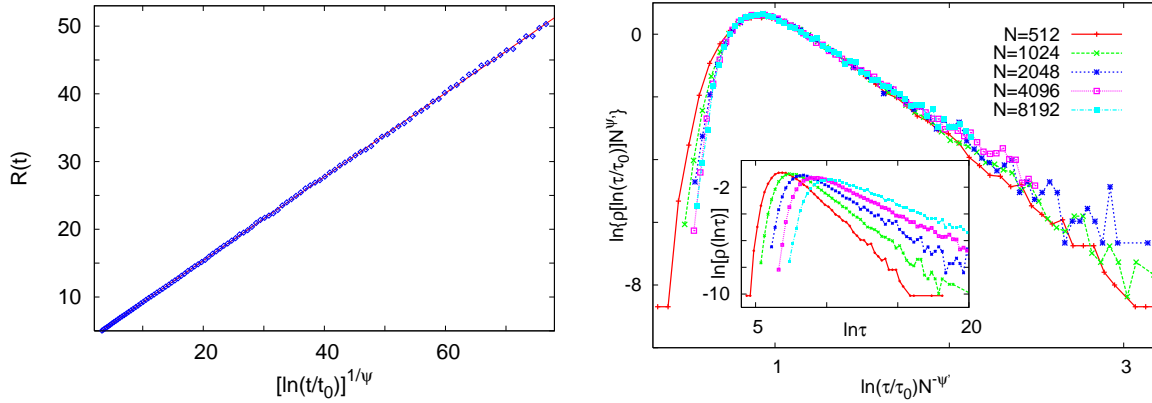


Figure 7. Left: Time-dependence of the spread measured in numerical simulations for $\beta = 1$, at $\lambda = 3.410$. The solid line is a fit to the data, yielding the parameters $\ln t_0 = 2.4(4)$ and $\psi = 0.53(4)$. Right: Scaling collapse of the histogram of logarithmic lifetimes obtained for different sizes N . For each N , the lifetime has been measured in $10^4 - 10^5$ random samples, once in each sample. Optimal collapse is achieved by the parameters $\ln t_0 = 3$, $\psi' = 0.23$. The inset shows the unscaled histograms.

model with parameter disorder. The obtained estimates are shown in the last three columns of Table 2.

6. Discussion

We have studied the critical contact process and the slightly different SIS model in the presence of parameter disorder on finite-dimensional random LRC networks by an SDRG method and by Monte Carlo simulations. We have seen by both methods that the behavior of different observables are compatible with the scaling laws in infinite randomness fixed points and have obtained estimates of the critical exponents. As can be seen in Fig. 9, they vary smoothly with the graph dimension of networks. We have

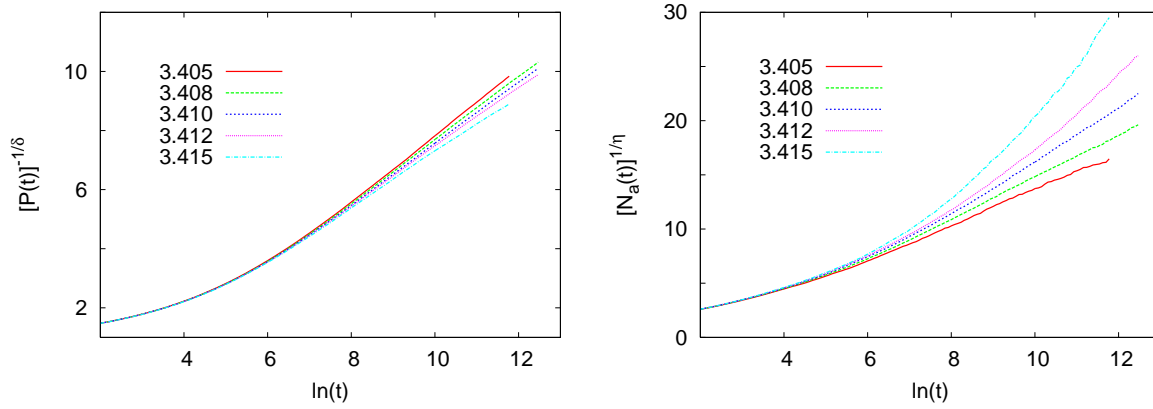


Figure 8. Time-dependence of the survival probability and the average number of active nodes for $\beta = 1$. According to Eqs. (12,13), the asymptote of the critical curve must be a line. The estimates of the critical exponents $\bar{\delta} = 1.94$, $\bar{\eta} = 0.54$ have been calculated from the data in Table 2 using Eq. (15).

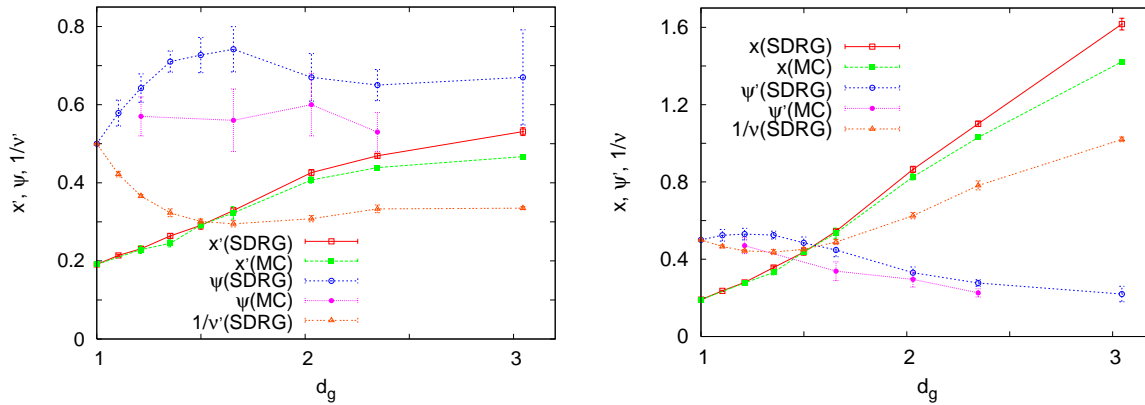


Figure 9. Estimates of different exponents plotted against the graph dimension.

observed the infinite-randomness scenario all the way to the largest value of d_g considered in this work and, taking into account the smooth change of critical exponents with d_g we conjecture this scenario to persist to arbitrarily large, finite graph dimensions.

In addition to the model with parameter disorder we performed simulations of the model with homogeneous parameters. Comparing the estimates of the critical exponents obtained in the two cases (see Table 2) we can see that they agree within the error of measurements. This suggests that, at least in the model under study, the presence of an additional parameter disorder does not alter the critical exponents of the infinite randomness fixed point induced solely by the topological disorder. For supporting this finding, a non-rigorous argument based on the SDRG approach of the problem can be provided, as follows.

Let us consider the SIS model and the contact process without parameter disorder. All recovery rates are now equal and, in the former, even the infection rates are uniform. The SDRG procedure, as formulated for parameter disorder, investigates small blocks

(consisting of two nodes in case of the fusion step) and tries to replace them by a single effective node. The success of the method lies (among others) in that a *local control parameter*, which is determined by the relative magnitude of local recovery and infection rates within the blocks exists. This is much different for topological disorder. Here, the locally supercritical regions are expected to be those sub-graphs which have an over-average number of internal links. These regions cannot be detected simply by investigating and reducing two-node blocks sequentially in the way the procedure works for parameter disorder. Instead larger blocks (at least three nodes) should be investigated so that the clusters which are super-critical due to the large number of internal links can be found §. Such a hypothetical SDRG method would be certainly much more complicated than the naive one but the difficulties are merely of technical nature and not principal ones. So we can assume that a renormalization procedure exists by which richly linked sub-graphs are selected and replaced by a single node with a properly calculated effective recovery rate. Obviously, the application of this pre-renormalization leads to that parameters of the model become disordered. In other words, we expect the topological disorder of the original model inducing parameter disorder in the coarse-grained (renormalized) model. Performing the hypothetical SDRG method up to a finite length scale, the resulting coarse-grained model will therefore be suitable for an SDRG analysis by the naive method developed for parameter disorder. Considering that the pre-renormalization carried out up to a finite-scale does not influence the asymptotical properties of the geometry of the underlying network and keeping in mind the universality in an IRFP, we conclude that the additional parameter disorder will not alter the critical behavior with respect to those induced by the topological disorder.

Let us now return to the comparison of the SDRG and Monte Carlo results. Concerning the exponent x' , the data obtained by the two methods are close to each other for small d_g but the deviation is significant and increasing for larger d_g , see Fig. 6. However, for larger d_g , the effective strength of disorder is weaker, which manifests itself in that $\psi'(d_g)$ is decreasing with d_g , and this makes the estimates by both methods less reliable for larger graph dimensions. Regarding that the agreement is quite good for moderate d_g , we conjecture that both models are in the same universality class for any d_g and attribute the discrepancy for larger d_g to possible systematic errors related to the finite size of networks used in the numerical analysis ||. As can be seen in Fig. 9, the exponents x' and ν' vary with the graph dimension slowly for large d_g and the exponents ν' fulfill the rigorous bound $\nu' \geq 2$ for all d_g [47]. The dependence of these exponents on d_g is similar to that on the dimension in hypercubic lattices [25].

The tunneling exponent ψ is found to saturate for large graph dimensions according to both methods, see Table 1 and 2, although the values obtained by the SDRG

§ This problem also arises in the case of the contact process on diluted hypercubic lattices. Dilution and parameter disorder have been observed to be in the same universality class [45].

|| Note that deviations between the SDRG and Monte Carlo estimates have been established also in the case of the contact process on hypercubic lattices with parameter disorder [46].

method are systematically higher than those obtained by Monte Carlo simulations. For the exponent ψ , one can easily establish an upper bound for arbitrary β , as follows. According to Eq. (14), the exponent ψ' governs the scaling of the typical time t during which the activity spreads (in surviving trials) in a finite sample of size N from the origin to the node in the Euclidean distance $N/2$, through $\ln t \sim N^{\psi'}$. Furthermore, increasing β amounts to that the number of long links increases in the network. Then, it is plausible to assume that the time t must not increase with increasing β since the long edges promote the spreading of activity. Consequently, the exponent $\psi'(\beta)$ must not increase with β . Since $\psi'(\beta = 0) = 1/2$, it follows that

$$\psi'(\beta) \leq 1/2 \quad (24)$$

for any β .

As can be seen from the data, the decreasing tendency of $\psi'(\beta)$ and the above inequality are fulfilled except of the SDRG estimates for small values of β ; nevertheless, the upper bound lies within the error of estimates also here. This may be attributed to the relatively strong finite-size corrections, depending heavily on the chosen distribution of the parameters. In order to have more accurate results, even larger system sizes should be needed, or, possibly, other forms of disorder, where the finite-size corrections have a different sign.

It is interesting to note that the possible saturation of ψ with increasing dimension has been observed also on hypercubic lattices, although to a value (0.46) lower than that obtained by either methods of this work on LRC networks [25].

The exponents describing the critical dynamics of the contact process, $\bar{\delta}$ and $\bar{\eta}$, can be calculated from the data in Table 1 and 2. Both vary with the graph dimension, the former increasing, the latter decreasing with d_g , in agreement with the tendencies on hypercubic lattices.

7. Conclusions and outlook

We have studied in this work the contact process, as well as the SIS model on LRC networks, where the topological disorder leads to infinite-randomness critical behavior. We have found by a numerical analysis supported by heuristic argumentations, that an additional parameter disorder does not change the critical exponents of the transition. In this way, the exponents are universal in the sense that they are determined exclusively by the topology of the network. This result opens up an alternative way of investigating infinite randomness critical behavior induced by topological disorder in general. Namely, after introducing parameter disorder, which is irrelevant in the above sense, one can apply the efficient SDRG method to the model.

Furthermore, the present numerical study has shown that in the case it is questionable whether the phase transition in a given model is of IRFP type or conventional one, it is better to concentrate on the critical behavior rather than searching for a Griffiths phase (an accompaniment of IRFP), which may be, in case of a relatively weak disorder (small ψ'), very hard to detect.

We have clearly seen in the present work, that the critical exponents smoothly vary with the topological dimension and, for moderate values of d_g we provided estimates on them. We have obtained from these data indications on the possible limiting behavior of these exponents when $d_g \rightarrow \infty$. Although the exponents for finite d_g does not seem to be determined exclusively by d_g (cf. the estimates on hypercubic lattices [25]), it is an intriguing question whether the limiting values of them are universal for $d_g \rightarrow \infty$. In a wider context, it is also a challenging question, whether there are such topological characteristics of the underlying networks which determine the critical exponent of the IRFP on the top of them unambiguously or at least approximately.

As mentioned in the Introduction, the transverse-field Ising model is in the same universality class as the contact process, in the presence of parameter disorder. Our results indicate that the critical behavior of the above model defined on LRC networks where there is exclusively topological disorder would be also described by an IRFP characterized by critical exponents obtained in the present work.

Acknowledgments

This work was supported by the János Bolyai Research Scholarship of the Hungarian Academy of Sciences, by the National Research Fund under grant no. K75324, and partially supported by the European Union and the European Social Fund through project FuturICT.hu (grant no.: TAMOP-4.2.2.C-11/1/KONV-2012-0013).

References

- [1] Barthelemy M, Barrat A, and Vespignani A 2008 *Dynamical processes on complex networks* (Cambridge Univ. Press, Cambridge)
- [2] Dorogovtsev S N, Goltsev A V, Mendes J F F 2008 Rev. Mod. Phys. **80** 1275
- [3] Albert R, Barabási A L 2002 Rev. Mod. Phys. **74** 47
- [4] Watts D J and Strogatz S H 1998 Nature **393** 440
- [5] Newman M E J 2000 J. Stat. Phys. **101** 819
- [6] Pastor-Satorras R, Vespignani A 2001 Phys. Rev. Lett. **86** 3200; 2001 Phys. Rev. E **63** 066117; Castellano C, Pastor-Satorras R 2006 Phys. Rev. Lett. **96** 038701; 2007 Phys. Rev. Lett. **98** 029802; 2008 Phys. Rev. Lett. **100**, 148701; Ha M, Hong H, Park H 2007 Phys. Rev. Lett. **98** 029801
- [7] Harris T E 1974 Ann. Prob. **2** 969
- [8] Muñoz M A , Juhász R, Castellano C, Ódor G, 2010 Phys. Rev. Lett. **105** 128701
- [9] Ódor G, Juhász R, Castellano C, Muñoz M A, 2011 AIP. Conf. Proc. **1332** 172
- [10] Juhász R, Ódor G, Castellano C, Muñoz M A 2012 Phys. Rev. E **85** 066125
- [11] Lambiotte R, Blondel V D, de Kerchove C, Huens E, Prieur C, Smoreda Z, Van Dooren P, 2008 Physica A **387** 5317
- [12] Bianconi G, Pin P, Marsili M 2009 Proc. Natl. Acad. Sci. **106** 11433
- [13] Benjamini I, Berger N 2001 Rand. Struct. Alg. **19** 102
- [14] Coppersmith D, Gamarnik D, Sviridenko M 2002 Rand. Struct. Alg. **21** 1
- [15] Juhász R 2012 Phys. Rev. E **85** 011118
- [16] Marro J, Dickman R 2005 *Non-equilibrium phase transitions in lattice models* Cambridge Univ. Press, Cambridge

- [17] Henkel M, Hinrichsen H, Lübeck S 2008 *Non-equilibrium Phase transitions* Springer, Berlin
- [18] Ódor G 2008 *Universality in Nonequilibrium Lattice Systems* World Scientific; 2004 Rev. Mod. Phys. **76** 663
- [19] Griffiths R B 1969 Phys. Rev. Lett. **23** 17; McCoy B M 1969 Phys. Rev. Lett. **23** 383
- [20] Noest A J 1986 Phys. Rev. Lett. **57** 91; 1988 Phys. Rev. **B 38** 2715; Cafiero R, Gabrielli A, Muñoz M A 1998 Phys. Rev. E. **57** 5060
- [21] Moreira A G, Dickman R 1996 Phys. Rev. E **54** R3090
- [22] Hooyberghs J, Iglói F, Vanderzande C 2003 Phys. Rev. Lett. **90** 100601; 2004 Phys. Rev. E **69** 066140
- [23] For a review, see Iglói F, Monthus C 2005 Phys. Rep. **412** 277
- [24] Erdős P, Rényi A 1959 Publicationes Mathematicae **6** 290
- [25] Kovács I A, Iglói F 2010 Phys. Rev. B **82** 054437; 2011 Phys. Rev. B **83** 174207
- [26] Kovács I A, Iglói F 2011 J. Phys.: Condens. Matter **23** 404204
- [27] Monthus C, Garel T 2012 J. Stat. Mech. P01008; 2012 J. Stat. Mech. P09016
- [28] Kovács I A 2012 PhD thesis, Eötvös Loránd University, Budapest, Hungary.
- [29] Kovács I A, Iglói F 2009 Phys. Rev. B **80**, 214416
- [30] Fisher D S 1992 Phys. Rev. Lett. **69** 534; 1995 Phys. Rev. B **51** 6411
- [31] Dutta A, Loganayagam R 2007 Phys. Rev. B **75** 052405
- [32] Chakrabarti B K, Maggs A C, Stinchcombe R B 1985 J. Phys. A: Math. Gen. **18** L373; Chowdhury D, Chakrabarti B 1985 J. Phys. A: Math. Gen. **18** L377
- [33] Kleinberg J M 2000 Nature **406** 845
- [34] Leuzzi L, Parisi G, Ricci-Tersenghi F, Ruiz-Lorenzo J J 2008 Phys. Rev. Lett. **101** 107203; Beyer F, Weigel M, Moore M A 2012 Phys. Rev. B **86** 014431
- [35] Aizenman M, Newman C M 1986 Commun. Math. Phys. **107** 611
- [36] Jespersen S, Blumen A 2000 Phys. Rev. E **62** 6270; Berger N 2002 Commun. Math. Phys. **226** 531;
- [37] Khaleque A, Sen P 2013 J. Phys. A: Math. Theor. **46** 095007
- [38] Grassberger P arXiv:1212.5396
- [39] Sen P, Chakrabarti B 2001 J. Phys. A: Math. Gen. **34** 7749
- [40] Moukarzel C F, Argollo de Menezes M 2002 Phys. Rev. E **65** 056709
- [41] Biskup M 2004 Ann. Probab. **32** 2933
- [42] Daqing L, Kosmidis K, Bunde A, Havlin S 2011 Nature Physics **7** 481; Emmerich T, Bunde A, Havlin S, Guanlian L, Daqing L arXiv:1206.5710
- [43] Batagelj V, Mrvar A 1998 Connections **21** 47
- [44] Juhász R 2013 Phys. Rev. E **87** 022133
- [45] Vojta T, Farquhar A, Mast J 2009 Phys. Rev. E **79** 011111
- [46] Vojta T 2012 Phys. Rev. E **86** 051137
- [47] Chayes J T, Chayes L, Fisher D S, Spencer T 1986 Phys. Rev. Lett. **57** (24):29993002